Wave height guided multi-shot receiver deghosting

Gordon Poole and Simon King, CGG

Summary

Many hydrophone only receiver deghosting algorithms make a flat sea surface assumption. In the case of significant ocean swell a variable free-surface datum is imposed and this assumption will not be met, resulting in degraded results. We extend a multi-shot receiver deghosting approach that satisfies the recorded primary and ghost wavefields by incorporating the presence of a variable free-surface at the source and receiver sides. The approach derives a τ-p_{sht}-p_{rec} model of the data at mean free-surface datum to estimate and remove the ghost. The approach is shown to produce high resolution receiver deghosting results with improved spatial consistency on a variable-depth streamer dataset from the North Sea.

Introduction

In a marine setting seismic measurements are affected by acquisition factors such as array effects as well as environmental factors such as free-surface ghosts. Free-surface ghosts limit the usable bandwidth of raw recordings by introducing notches in the frequency spectrum. The notch positions are a function of the propagation angle, source and receiver depth, and local free-surface datum or wave height (King and Poole, 2015). Ideally all these factors should be addressed in processing to reveal an accurate image of the Earth response.

On the source side broadband processing flows have modified traditional debubble/zero phase designature to include source deghosting so as to widen the bandwidth. On the receiver side several methods have been described to perform deghosting. These include the use of over-under streamers (Sønneland et al., 1986), dual-sensor streamers (Carlson et al., 2007) and variable-depth streamers (Soubaras, 2010; Poole, 2013; Wang et al., 2013).

King and Poole (2015) show that, instead of using a horizontal free-surface assumption, use of wave height information can improve the fidelity of high frequencies after receiver deghosting. Poole et al. (2016) show how spatially consistent deghosting may be achieved with use of the joint shot-receiver domain.

In this paper we introduce wave height information into the joint shot-receiver domain deghosting approach and demonstrate the benefits on a North Sea dataset.

Methodology

Poole et al. (2016) show how receiver deghosting working on a group of shots at the same time can be more robust to noise and provide more spatially consistent results than shot-by-shot deghosting. Simplifying the notation of Poole et al. (2016), and with the assumption of 2D wavefield propagation, we state the receiver ghost equation in the frequency domain as:

$$d_{sr}(n) = L_{sr}(n,m)p_{sr}(m) \quad (1)$$

where operator L_{sr} is defined by:

$$L_{sr} = e^{-2\pi i f x s_{sx}}\left[e^{-2\pi i f \tau_{\mathrm{p}}} + Re^{-2\pi i f \tau_{\mathrm{g}}}\right] \quad (2)$$

$$\tau_{\mathrm{p}} = xs_{rx} - zs_{rz} \quad (3)$$

$$\tau_{\mathrm{g}} = xs_{rx} + zs_{rz} \quad (4)$$

In this notation, d_{sr} is the input data, p_{sr} is the τ-p_{sht}-p_{rec} model of surface datum ghost free energy to be found by inversion, f is frequency (*Hz*), x is the offset of a given trace (*m*), s_{sx} and s_{rx} are model domain slownesses ($s.m^{-1}$) along the shot and receiver axes respectively, τ_{p} and τ_{g} relate to the timings of primary and ghost wavefields respectively (*s*), z is the receiver depth of a given trace (*m*), and given the water velocity, v_w ($m.s^{-1}$), vertical slowness may be computed using the expression $\frac{1}{v_w^2} = s_{rx}^2 + s_{rz}^2$. The bracketed exponential terms in equation 2 encode the receiver ghost with surface reflectivity, R (usually *-1*), as well as applying the reverse τ-p transform in the shot domain. The exponential outside the bracket performs the reverse τ-p transform in the receiver domain.

Ocean swell variations modify the free-surface datum above the streamers which will vary as a function of time and space. These variations will perturb the timing of the free-surface receiver ghost as illustrated in Figure 1. Figure 2 shows consecutive shots after 1D source designature including source ghost compensation followed by water velocity NMO. The receiver ghost following the water-bottom reflection is highlighted by the arrows. The variable receiver ghost timing due to the changing wave height

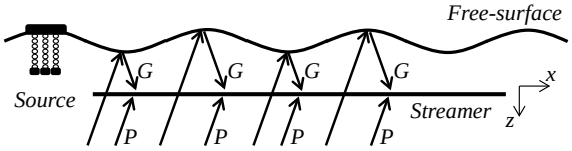

Figure 1: Illustration of the variation in receiver ghost timing due to a variable free-surface datum. *P* and *G* represent primary and ghost arrivals.

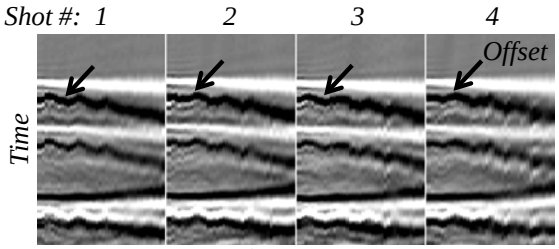

Figure 2: Consecutive shots after water velocity normal moveout.

above the streamer can clearly be seen to change on a shot-by-shot basis. In this example the shooting interval was approximately 10 s, and ocean swell variation was in the order of ±2 m in height with a spatial wavelength of 100 m.

An air-gun source acquisition scenario for two shots is illustrated in Figure 3 where three air-guns are suspended from a gun float. As the air-guns are suspended from the gun float by chains, they will be at a fixed depth from the local free-surface. For this reason the source ghost delay will be approximately constant relative to the primary. However, wave height variations on the source side will result in a shot-to-shot variation in timing of the signal recorded at the receiver. Referring to Figure 3, the signal from *Shot 1* will be delayed relative to the signal from *Shot 2* due to being at a higher elevation. Figure 4 shows a common channel after receiver deghosting but before source designature. Shot-to-shot time shifts may be seen on the reflections that affect both the primary (initial white event at the water bottom) as well as the source ghost (following black event).

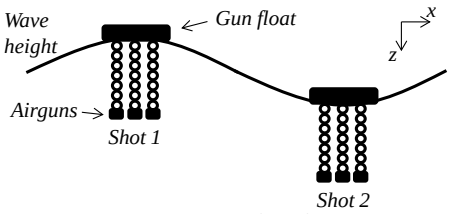

Figure 3: Air-gun source suspended from floats.

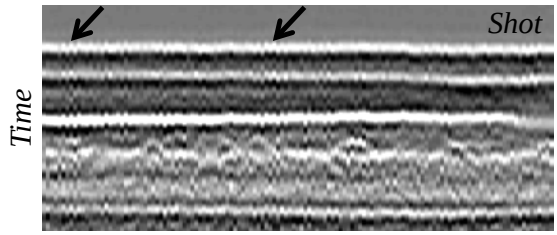

Figure 4: Common channel display.

The receiver side wave height may be derived from low-frequency hydrophone data (Kragh et al., 2002) or by cross-correlating recorded data with primary re-datumed data (assuming horizontal free-surface) as described by King and Poole (2015). The source side wave height may be found using GPS measurements, the high spatial frequency component of the water-bottom reflection time, or by shot-to-shot cross-correlation picking.

Given source and receiver wave height information, d_s and d_r respectively (m), we may modify equations 2 and 4 to account for associated timing variations in primary and ghost arrivals:

$$L_{sr}^{wh} = e^{-2\pi i f(xs_{sx}+d_s s_{sz})}\left[e^{-2\pi i f \tau_p} + Re^{-2\pi i f \tau_g^{wh}}\right] \quad (5)$$

$$\tau_g^{wh} = xs_{rx} + (z + d_r)s_{rz} \quad (6)$$

On the receiver side a ghost delay equal to the receiver wave height, d_r, multiplied by the vertical slowness at the receiver side, s_{rz}, has been added. Similarly, the source correction has been included through multiplication of the source wave height, d_s, by the vertical slowness at the source side, s_{sz}.

The model, p_{sr}, may be found by solving equation 1 (for example using conjugate gradients) following which it may be used either to output primary data directly, or preferably to output a ghost model which may be subtracted from the input data. The approach may be applied in time windows, thus allowing the wave height to vary as a function of time.

Due to spatial aliasing relating to the shot sampling it will often be necessary to find the model, p_{sr}, using iteratively re-weighted least squares inversion (Trad et al., 2003) using low frequency information to dealias the high frequencies (Herrmann et al., 2000).

The formulations given above may be modified for the case of multi-sensor receivers (for example following, Poole, 2014 or Wang et al., 2014). Based on Poole et al. (2013) the equations may be modified to compensate for shot-to-shot directional source signature variations. While described in 2D, it should be noted that the equations may be extended to 3D where sampling allows.

Real data example

Receiver deghosting was performed on a real dataset from a towed streamer acquisition in the Norwegian North Sea. The broadband acquisition utilized 12 variable-depth streamers towed with a 75 m separation. The data was acquired using multi-level sources at 6 m and 9 m (Siliqi et al., 2013). Source ghost compensation was applied with a 1D debubble and ghost compensation filter, following which receiver deghosting was applied.

Figures 5a, 5b and 5c show a shot gather before and after water velocity NMO correction and a common channel gather prior to receiver deghosting, respectively. Arrows on the shot gathers illustrate the variable timing of the ghost relating to the wave height variations. Figures 5d, 5e and 5f show the corresponding data after shot-by-shot deghosting assuming a horizontal free-surface following Poole (2013). While the receiver deghosting has been broadly effective, the true character of the ghost has not been correctly modelled causing residual ghost to be observed at the position of the arrows. Data after shot-by-shot receiver deghosting using wave height information (following King and Poole, 2015) is given in Figures 5g, 5h, and 5i where the residual ghost is less prevalent and the high frequency clarity of the shallow section has been improved.

Figure 6a shows 10 Hz filter panels up to 50 Hz for a shot gather before receiver deghosting. Figures 6b and 6c show the corresponding filter panels after shot-by-shot receiver

deghosting and multi-shot receiver deghosting, respectively. Wave height information has been incorporated into both deghosting results so as to compare the approaches of shot-by-shot and multi-shot deghosting only. The arrows in Figure 6b highlight noise that stands out after shot-by-shot receiver deghosting. The noise is significantly reduced in Figure 6c after the proposed multi-shot receiver deghosting approach.

Figure 7a displays a zoom of the migration stack before receiver deghosting. Figures 7b and 7c illustrate the migration stack after shot-by-shot receiver deghosting assuming horizontal free surface and after the proposed multi-shot receiver deghosting using wave height information, respectively. Figure 7d shows the difference between the two deghosting approaches. It is clear that by incorporating wave height information along with multi-shot receiver deghosting, we achieve an image with less residual ghost at the water bottom and better spatial consistency in the faulted region as highlighted by the arrows in the migration difference.

Conclusions

Receiver deghosting algorithms may be less effective given the assumption of a horizontal free surface. We have extended a multi-shot receiver deghosting approach to utilize wave height information. The approach derives a model representation of mean free-surface datum ghost free data in the joint shot-receiver domain. The model is used to estimate a ghost wavefield that is subtracted from the input data. We have highlighted the benefits of the approach using data from a towed streamer acquisition in the North Sea. By incorporating wave height information into the joint shot-receiver deghosting approach, we observe less residual ghost whilst benefitting from improved spatial consistency in the final receiver deghosting results.

Acknowledgements

We thank CGG data library for the Northern Viking Graben data examples and CGG for permission to publish this work. We also thank Richard Wombell, James Cooper and CGG Subsurface Imaging help preparing the paper.

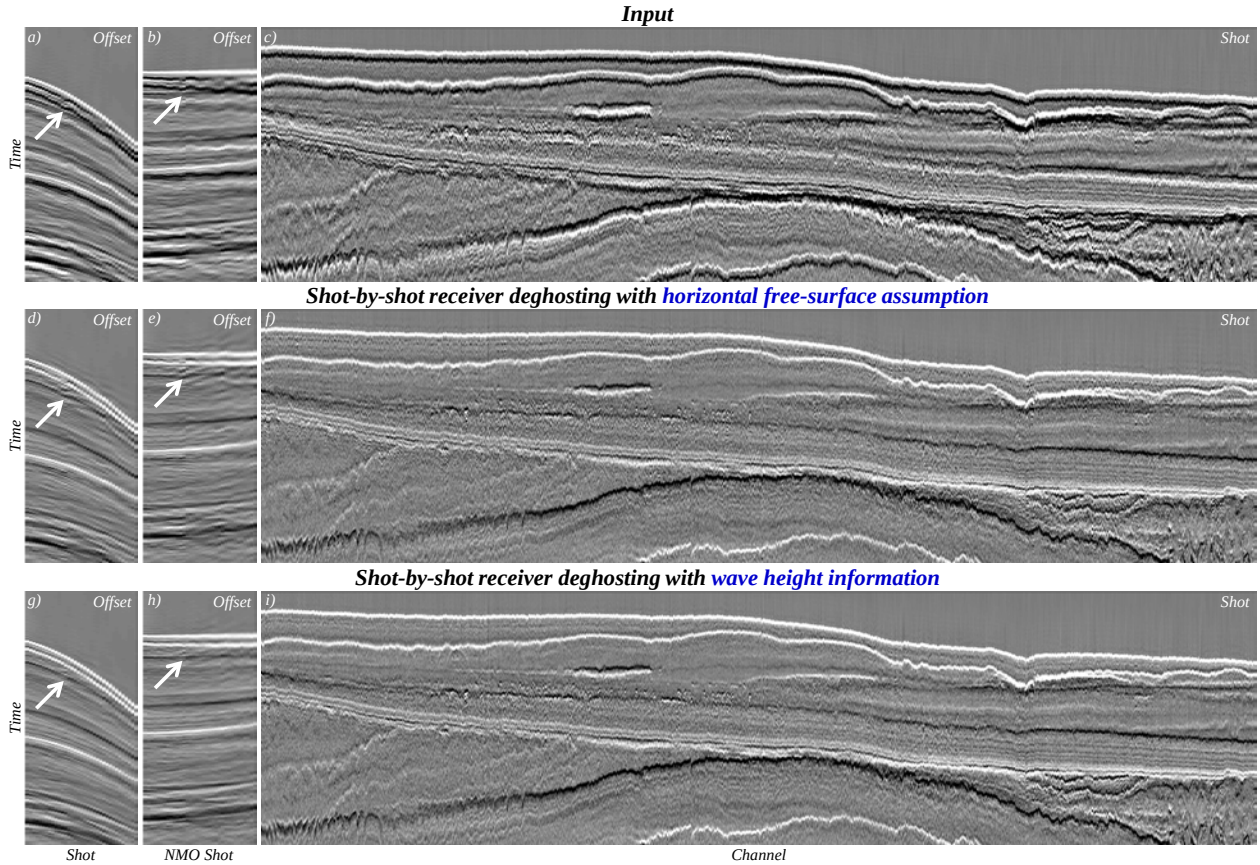

Figure 5: a) Shot, b) NMO shot and c) common channel before receiver deghosting. d), e), and f) corresponding plots after shot-by-shot receiver deghosting assuming horizontal sea surface. g), h), and i) corresponding plots after shot-by-shot receiver deghosting with wave height information.

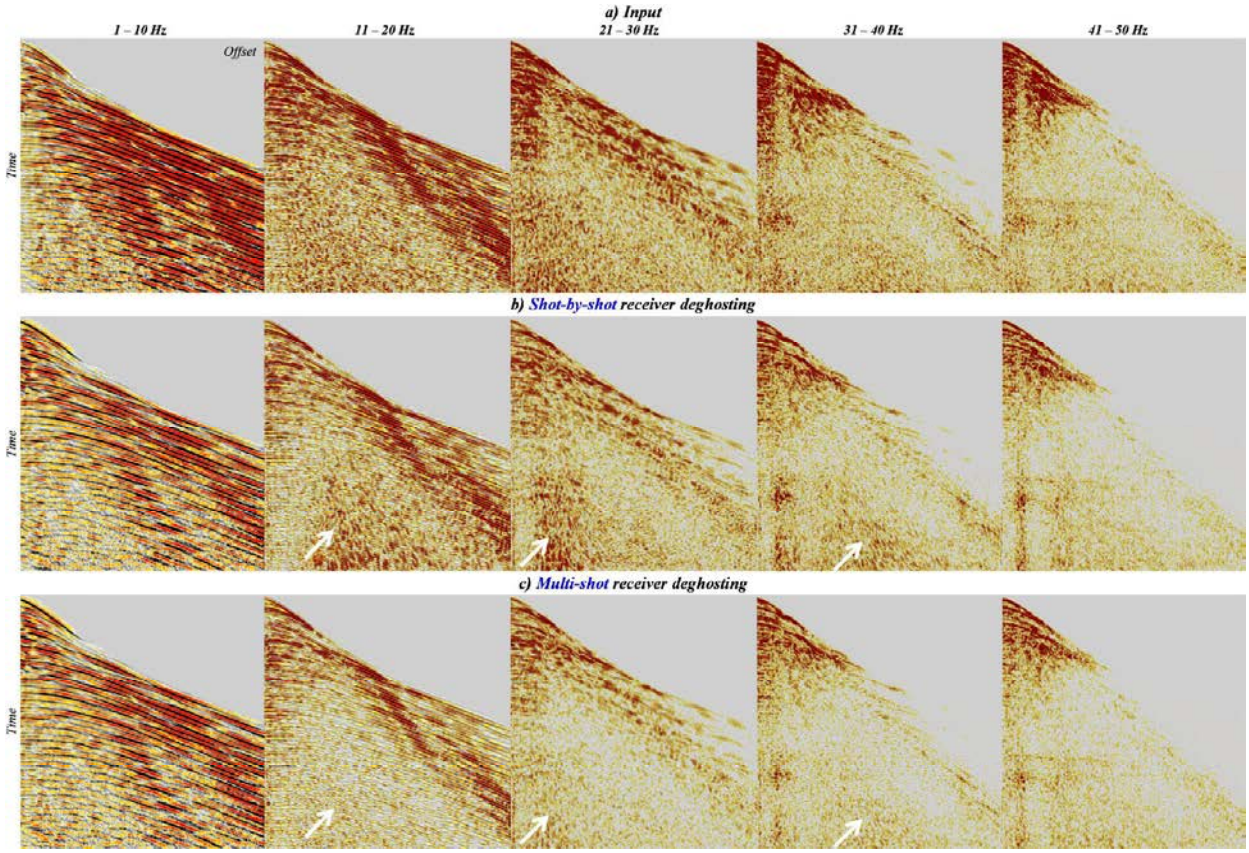

Figure 6: Shot gather filter panels a) before receiver deghosting, b) after shot-by-shot receiver deghosting and c) after multi-shot receiver deghosting. Both receiver deghosting methods used wave height information.

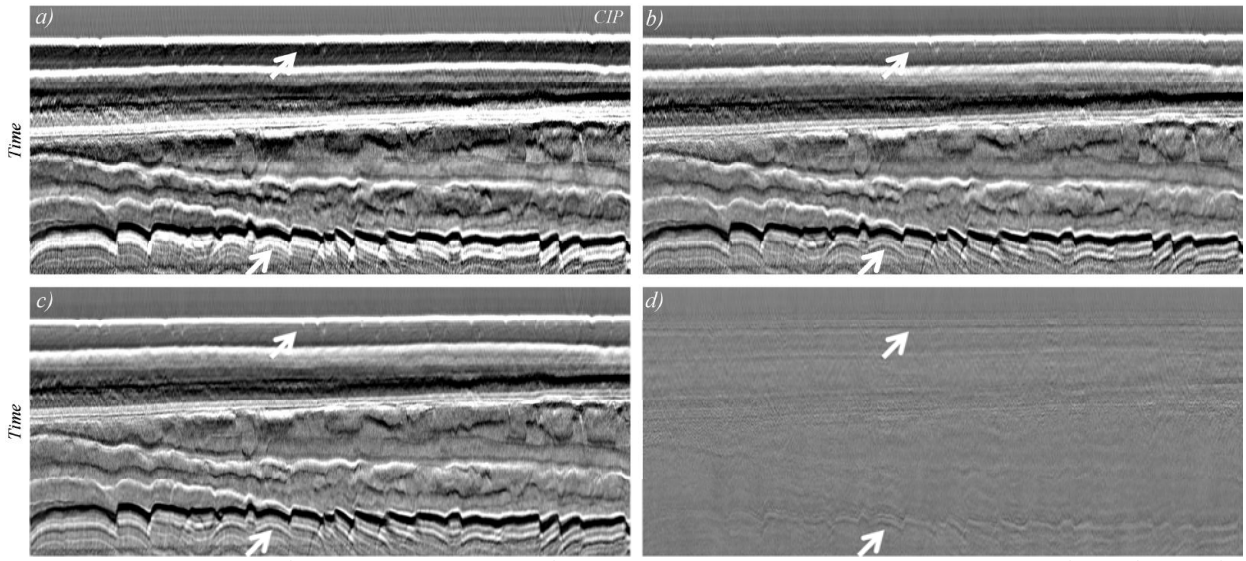

Figure 7: Migrated stacks a) before receiver deghosting, b) after shot-by-shot receiver deghosting assuming horizontal free surface, c) after multi-shot receiver deghosting with wave height information and d) the difference between b) and c).

EDITED REFERENCES

Note: This reference list is a copyedited version of the reference list submitted by the author. Reference lists for the 2016 SEG Technical Program Expanded Abstracts have been copyedited so that references provided with the online metadata for each paper will achieve a high degree of linking to cited sources that appear on the Web.

REFERENCES

Carlson, D., A. Long, W. Söllner, H. Tabti, R. Tenghamn, and N. Lunde, 2007, Increased resolution and penetration from a towed dual-sensor streamer: First Break, **25**, 71–77.

Herrmann, P., T. Mojesky, M. Magesan, and P. Hugonnet, 2000, De-aliased, high-resolution Radon transforms: 70th Annual International Meeting, SEG, Expanded Abstracts, 1953–1956, http://dx.doi.org/10.1190/1.1815818

King, S., and G. Poole, 2015, Hydrophone only receiver deghosting using a variable sea surface datum: 85th Annual International Meeting, SEG, Expanded Abstracts, 4610–4614, http://dx.doi.org/10.1190/segam2015-5891123.1.

Kragh, E., R. Laws, and L. Combee, 2002, Sea surface shape derivation above the seismic streamer: 64th Annual International Conference and Exhibition, EAGE, Extended Abstracts, A07.

Poole, G., 2013, Pre-migration receiver de-ghosting and re-datuming for variable depth streamer data: 83rd Annual International Meeting, SEG, Expanded Abstracts, 4216–4220, http://dx.doi.org/10.1190/segam2013-0541.1.

Poole, G., 2014, Wavefield separation using hydrophone and particle velocity components with arbitrary orientation: 84th Annual International Meeting, SEG, Expanded Abstracts, 1858–1862, http://dx.doi.org/10.1190/segam2014-0756.1.

Poole, G., C. Davison, J. Deeds, K. Davies, and G. Hampson, 2013, Shot-to-shot directional designature using near-field hydrophone data: 83rd Annual International Meeting, SEG, Expanded Abstracts, 4236–4240, http://dx.doi.org/10.1190/segam2013-0550.1.

Poole, G., S. King, and J. Cooper, 2016, Simultaneous source designature and receiver deghosting in the joint shot-receiver domain: 78th Annual International Conference and Exhibition, EAGE, Expanded Abstracts

Siliqi, R., T. Payen, R. Sablon, and K. Desrues, 2013, Synchronized multi-level source, a robust broadband marine solution: 83rd Annual International Meeting, SEG, Expanded Abstracts, 56–60, http://dx.doi.org/10.1190/segam2013-0966.1.

Sønneland, L., L. Berg, P. Eidsvig, A. Haugen, B. Fotland, and I. Vestby, 1986, 2D deghosting using vertical receiver arrays: 56th Annual International Meeting, SEG, Expanded Abstracts, 516–519.

Soubaras, R., 2010, Deghosting by joint deconvolution of a migration and a mirror migration: 80th Annual International Meeting, SEG, Expanded Abstracts, 3406–3410, http://dx.doi.org/10.1190/1.3513556.

Trad, D., T. Ulrych, and M. Sacchi, 2003, Latest views of the sparse Radon transform: Geophysics, **68**, 386–399, http://dx.doi.org/10.1190/1.1543224.

Wang, P., H. Jin, C. Peng, and S. Ray, 2014, Joint hydrophone and accelerometer receiver deghosting using sparse Tau-P inversion. 84th Annual International Meeting, SEG, Expanded Abstracts, 1894–1898, http://dx.doi.org/10.1190/segam2014-0865.1.

Wang, P., S. Ray, C. Peng, Y. Li, and G. Poole, 2013, Premigration deghosting for marine streamer data using a bootstrap approach in tau-p domain: 83rd Annual International Meeting, SEG, Expanded Abstracts, 4221–4225, http://dx.doi.org/10.1190/segam2013-0225.1.